Third-harmonic generation from Mie-type resonances of isolated all-dielectric nanoparticles

Elizaveta V. Melik-Gaykazyan,[†] Maxim R. Shcherbakov,[†] Alexander S. Shorokhov,[†] Isabelle Staude,[‡] Igal Brener,[¶] Dragomir N. Neshev,[‡] Yuri S. Kivshar,[‡] and Andrey A. Fedyanin[*,†]

Faculty of Physics, Lomonosov Moscow State University, Moscow 119991, Russia, Nonlinear Physics Centre, Research School of Physics and Engineering, The Australian National University, Canberra ACT 0200, Australia, and Center for Integrated Nanotechnologies, Sandia National Laboratories, Albuquerque, New Mexico 87185, United States

E-mail: fedyanin@nanolab.phys.msu.ru

Keywords: Nonlinear optics, third-harmonic generation, silicon nanodisks, optical magnetism, Mie scattering

Abstract

Subwavelength silicon nanoparticles are known to possess a set of strongly localized modes, including those with resonant electric and magnetic dipolar polarizabilities. Here we com-

[*]To whom correspondence should be addressed

[†]Faculty of Physics, Lomonosov Moscow State University, Moscow 119991, Russia

[‡]Nonlinear Physics Centre, Research School of Physics and Engineering, The Australian National University, Canberra ACT 0200, Australia

[¶]Center for Integrated Nanotechnologies, Sandia National Laboratories, Albuquerque, New Mexico 87185, United States

pare experimentally the third-harmonic generation efficiency from individual and uncoupled silicon nanodisks for resonant excitation at the Mie-type dipolar resonances. Using nonlinear spectroscopy, we observe that the fundamental magnetic dipolar mode yields efficient third-harmonic radiation in contrast to the electric dipolar mode. This is further supported by full-wave numerical simulations, where the volume-integrated local fields and the directly simulated nonlinear response are shown to be negligible at the electric dipolar resonance compared to the magnetic one.

Introduction

In nanoplasmonics, noble metal nanoparticles allow for shaping local electromagnetic fields on demand, an ability that has spawned many applications as well as inspired a vast amount of research in photonics.[1] Having control over the local fields is crucial for nonlinear-optical applications where frequency conversion, self-action and all-optical switching are highly sensitive to the structure geometry and the excited electromagnetic modes.[2] Apart from the electric dipolar (ED) modes in simple geometries like spheres[3,4] or dipole antennas,[5,6] the modes with considerable magnetic dipolar (MD) moment[7–9] were extensively studied in the nonlinear-optical regime.[10] For instance, efficient second- and third-harmonic (TH) response was found in split-ring resonators,[11] fishnet metamaterials,[12] split-hole cavities,[13] and nanosandwiches.[14] A special contribution of MD modes to the nonlinear multipolar response of metasurfaces was indicated.[14,15]

Observation of MD modes[16] in dielectric resonators[17] and in particular in silicon nanoparticles[18,19] was an important step towards low-loss nanophotonics.[20] Having extremely low absorption in the near-infrared spectral region, silicon is even more attractive in the nonlinear regime.[21,22] Previously, we have shown that MD modes can substantially improve the nonlinear response of silicon nanodisks[23,24] and their oligomers.[25] Apart from the fact that the MD mode is often the lowest-order mode of a high-index subwavelength spherical or disk-

like nanoparticle, it remained unclear whether there is any further advantage of utilizing this mode for nonlinear conversion processes as compared to other, higher-order modes.

In this paper, we compare the nonlinearities of optically isolated silicon nanoparticles when pumped at their electric and magnetic dipolar resonances by employing third-harmonic generation (THG) spectroscopy technique. As depicted schematically in Fig. 1(a), we observe that exciting the magnetic dipolar resonance leads to a large THG yield compared to the case of electric dipolar resonance because of the stronger field confinement within the nanodisk for the MD resonance. This is supported by rigorous numerical calculations of the electric field distributions that show strong enhancement of the overall local field for the magnetic dipole mode and by rigorous numerical simulations of the nonlinear-optical response.

Methods

Samples. Nanodisk arrays are fabricated starting with a silicon-on-insulator (SOI) wafer, produced by *Soitec*, using electron-beam lithography and reactive-ion etching processes. The top (100)-cut Si layer of the wafer is 260-nm-thick. We consider two square 400x400 μm^2 arrays distinguished by the disk diameter values of $d = 345$ and 360 nm, respectively. The nanodisk lattice spacing is $p = 2.85$ μm for all the diameters. As opposed to our previous results on nonlinear spectroscopy of Si metasurfaces,[23] such a period value allows for studying isolated nanodisks due to negligible optical coupling ($d \ll p$ and $\lambda < p$). The choice of the nanodisk diameter and height specifies the MD and ED resonance wavelengths.[26] A scanning electronic microscopy image of a 360-nm disk array part is shown in Fig. 1(b).

Nonlinear spectroscopy. In order to study the nonlinear-optical response of the nanodisks and to clarify the roles played by ED and MD resonances in the harmonic generation process, we conduct nonlinear THG spectroscopy measurements. An optical parametric oscillator (Angewandte Physik & Electronik GmbH OPO PP Automatic, 200 fs pulses) is pumped by a Ti:Sapphire oscillator (Coherent Chameleon Ultra II, repetition rate 76 MHz)

and tuned in the range of 1.0-1.5 μm. The beam polarization is conditioned by a pair of laser Glan prisms. The waist diameter is set at 11 μm by an aspherical lens. The beam is focused from the back of the sample, and the transmitted third-harmonic beam is measured. The full thickness of the SOI wafer (500 μm) is comparable to the waist depth. The resulting peak intensity reached the values of about 1 GW/cm^2 in the sample plane. For the preliminary focusing at the area of interest, a CCD-camera and a halogen lamp radiation are used. The transmitted and collimated THG signal is selected by a set of blue filters and detected by a photomultiplier tube connected to a lock-in amplifier. The periodic arrangement formed a square diffraction pattern; we deliberately collect only the zeroth transmitted order in order to measure the forward-scattered signal only. This signal is proven to be of the TH origin by checking its cubic dependence on the pump power and by direct measurements of its spectrum by a spectrometer. It has been also verified that the THG beam is polarized in parallel to the orientation of the pump beam polarization. It should be pointed out that the penetration depth of the THG into silicon does not exceed the nanodisk height.

The key feature of our approach is the possibility to cancel out all the sample-irrelevant contributions to the measured spectra, such as pulse duration and power variations, along with spectral features of the setup itself, as well as the dispersion of $\chi^{(3)}$ for bulk silicon. Our nonlinear spectroscopy setup has an option for measuring the linear transmittance spectra by focusing white light to a 20-μm-wide spot on the sample plane and consecutively measuring its spectrum using an IR-spectrometer. All measurements are carried out under normal incidence and with all the beams polarized along the side of the sample periodicity cell. The numerical aperture of our excitation train was equal to 0.15.

Estimation of third-harmonic output via local fields integration. The fact of the higher TH yield upon pumping the MD resonances if compared with the ED resonance is supported by estimating the overall nonlinear polarization within the nanodisks. This has been done by integrating the local fields over the volume of the nanodisk. To simulate the nanodisks response to external radiation we implement a model using *FDTD Solutions*

software by *Lumerical Solutions, Inc.* This model includes a plane wave pulse with the wide spectral range (0.8–1.4 μm) as an external radiation source located inside the silica substrate. For a Si nanodisk, dimensions are set equal to those of the experiment; namely, the height is 260 nm, and the diameter is 360 nm. After calculating the electromagnetic field components outside and inside the disk, we integrate the Cartesian components of the time-averaged electric field:

$$|E_{\mathrm{int},i}(\lambda)|^2 = \int\limits_{V_{\mathrm{disk}}} |E_i(\mathbf{r},\lambda)|^2 d\mathbf{r}, \tag{1}$$

and the absolute value of the squared total field:

$$|E_{\mathrm{int}}(\lambda)|^2 = \int\limits_{V_{\mathrm{disk}}} (|E_x(\mathbf{r},\lambda)|^2 + |E_y(\mathbf{r},\lambda)|^2 + |E_z(\mathbf{r},\lambda)|^2) d\mathbf{r}, \tag{2}$$

over the disk volume V_{disk}. The spectral features of the source are taken into account by a normalizaton procedure. The disk is considered isolated due to the perfectly matched layers set as boundary conditions.

Numerical simulations of third-harmonic output. Our nonlinear spectroscopy result is compared with direct numerical calculations of THG response. We consider the same model of the nanodisk on the silica substrate using *FDTD Solutions* software by *Lumerical Solutions, Inc.* The material of the disk was augmented by a constant isotropic nonlinear susceptibility $\chi^{(3)}$. For each wavelength, pump was simulated to be a plane wave pulse with a relatively narrow spectral width of 5 nm, which was close to the experimental value. Nonlinear signal was recorded in the spectral vicinity of the respective tripled frequency as detected by a two-dimensional transmission monitor and integrated as a function of the two coordinates and frequency.

Results and Discussion

The main experimental results of our study are shown in Fig. 2. For the linear optical response characterization, we normalize the white-light transmittance spectrum by the spectrum of the nearby substrate area measured under the same conditions. We observe two dips in the normalized transmittance spectra. The dips correspond to the electric dipolar resonance found at shorter wavelengths, and magnetic dipolar resonance found at longer wavelengths; this interpretation is supported by the corresponding numerical calculations summarized below. A difference in the position of the magnetic resonance wavelength observed for the two samples is about 30 nm, and this is more substantial for the magnetic rather than for electric resonance due to the sensitivity of the former to the disk diameter.[26]

The measured THG spectra are shown in Figs. 2(a,b) with black dots and corresponding error bars. First, despite the simultaneous illumination of both the nanodisk arrays and the bulk silicon SOI substrate, we observe a significant THG enhancement from the nanodisks compared to the bulk silicon THG. The enhancement peak corresponds to the wavelength of the MD resonance. Interestingly, the THG enhancement is highly pronounced at the MD resonance wavelength (this was observed in our previous work for optically coupled nanodisks too[23]) whereas at the ED resonance there is no any sufficient enhancement. The THG line is expectedly narrower than that of the transmittance spectrum. A small, yet persistent, red shift of the central THG resonance wavelength is observed with respect to the transmittance dip. The maximum enhancement defined as a ratio of the normalized THG signal to the inverse value of the relative nanodisk area is around 30, which is consistent with our previous findings for sparsely arranged oligomers.[25]

In order to elucidate the observed asymmetry in efficiencies between the third-harmonic generation at the magnetic resonance versus that at the electric resonance we calculate numerically the volume-integrated local electromagnetic fields within the disk. It is known that the nonlinear polarization depends strongly on the strength of the local electromagnetic

field; in the case of the scalar nonlinear susceptibility $\chi^{(3)}$ (see, e. g., Ref.[27]):

$$\tilde{P}(t) = \chi^{(3)} \tilde{E}^3_{\text{local}}(t). \tag{3}$$

Here, $\tilde{P}(t)$ is the induced third-order nonlinear polarization that results in TH radiation in the far field. Although the mechanism that leads to the resulting far-field THG pattern is complicated, here we rely on the assumption that the local field value E_{local} is the dominant mechanism for the overall TH response. First, using finite-difference time-domain (FDTD) approach we calculate $\mathbf{E}_{\text{local}}(\mathbf{r}, \lambda)$ maps within the single silicon nanodisk situated on a silica substrate. The dimensions of the nanodisks are taken from the experimental values (h = 260 nm, d = 360 nm). Then, the time-averaged fields are integrated over the volume of the nanodisk; the integrated values $\mathbf{E}_{\text{int}}(\lambda)$ give a direct estimate of how much TH should be detected at a particular pump wavelength λ. The spectra of the volume-integrated local fields are provided in Fig. 3. Here, the components and the absolute field value squared are plotted in the spectral range of three low-order Mie-type resonances that carry MD, ED and magnetic quadrupolar[18,19] (MQ) moments. From the spectra of the integrated local fields, it can be seen that the ED resonance has little contribution to the overall local field enhancement. The strongest nonlinear response is, therefore, expected at the MD and MQ resonances. This is also supported by the corresponding local field maps that are provided in Fig. 3 for MD at λ = 1.296 μm, for ED at λ = 1.03 μm and for MQ at λ = 0.896 μm. The largest local electric field value is obtained at the MQ resonance. If one compares the ED and MD modes, the peak local field values within the nanodisk are in favor of the MD resonance: the normalized E-field peaks at 2.71 at the ED resonance versus 3.20 at the MD resonance. Also, the overall volume covered by hotspots is visually larger for the MD mode. Therefore, the experimentally observed enhanced THG at the MD resonance as compared to the THG output at the ED resonance is can be validated by the simple local-field hypothesis. This observation makes MD resonances of high-index nanoparticles

very relevant to nonlinear-optical applications in nanophotonics.

Moreover, direct numerical simulations show that the THG response takes place at the MD resonance of an isolated silicon disk, while there is little nonlinear signal at the ED resonance pump frequency (Fig. 4). A significant enhancement of nonlinear processes efficiency is also predicted at the MQ resonance; an experimental verification of this fact could be interesting for ultraviolet photonics applications. An apparent red spectral shift of the TH signal with respect to the spectral position of the MD mode-associated dip is consistent with the integrated electric field in Fig. 3.

Conclusion

In summary, we have studied the third-harmonic response of silicon nanodisks at their electric and magnetic Mie-type dipolar resonances. The enhanced up-conversion efficiency at the magnetic dipolar resonance of the nanodisks has been observed due to the strong field confinement, whereas the electric dipolar resonance yielded almost no nonlinear conversion. The experimental findings have been supported by rigorous nonlinear numerical calculations, where considerably lower average local field density and overall THG has been detected at the electric resonance, as compared with the magnetic resonance. Our results provide an important step towards the better understanding of artificial resonant all-dielectric nanostructures and their nonlinear-optical response at the nanoscale.

Acknowledgements. The authors thank Ivan Iorsh and Daria Smirnova for fruitful discussions.

Funding. Financial support from Russian Science Foundation (Grant #14-12-01144, experimental part), Russian Foundation for Basic Research (calculations), and the Australian Research Council is acknowledged. This work was performed, in part, at the Center for Integrated Nanotechnologies, an Office of Science User Facility operated for the U.S. Department

of Energy (DOE) Office of Science. Sandia National Laboratories is a multiprogram laboratory managed and operated by Sandia Corporation, a wholly owned subsidiary of Lockheed Martin Corporation, for the U.S. Department of Energy's National Nuclear Security Administration under contract DE-AC04-94AL85000.

Competing Interests. The authors have no competing interests.

Authors' Contributions. All the authors contributed to conceptualizing this manuscript. EVM carried out numerical simulations and experiments. EVM and MRS wrote the first draft. EVM, MRS and ASS chose the methods and constructed the experimental setup. IS and IB fabricated the sample. IS, DNN, IB, YSK and AAF revised the manuscript. All the authors gave final approval for publication.

References

(1) Maier SA. 2007 Plasmonics: Fundamentals and applications. *Springer Science+Business Media New York: New York*.

(2) Kauranen M, Zayats AV. 2012 Nonlinear plasmonics. *Nature Photon.* **6**, 737–748. (doi:10.1038/nphoton.2012.244)

(3) Lippitz M, Dijk MA, Orrit M. 2005 Third-harmonic generation from single gold nanoparticles. *Nano Lett.* **5**, 799–802. (doi:10.1021/nl0502571)

(4) Liu TM, Tal SP, Yu CH, Wen YC, Chu SW, Chen LJ, Prasad MR, Lin KJ, Sun CK. 2006 Measuring plasmon-resonance enhanced third-harmonic $\chi(3)$ of Ag nanoparticles. *Appl. Phys. Lett.* **89**, 112–114. (doi:10.1063/1.2240738)

(5) Aouani H, Rahmani M, Navarro-Cía M, Maier SA. 2014 Third-harmonic-upconversion enhancement from a single semiconductor nanoparticle coupled to a plasmonic antenna. *Nat. Nanotechnol.* **9**, 290–294. (doi:10.1038/nnano.2014.27)

(6) Metzger B, Hentschel M, Schumacher T, Lippitz M, Ye X, Murray CB, Knabe B, Buse K, Giessen H. 2014 Doubling the efficiency of third harmonic generation by positioning ITO nanocrystals into the hot-spot of plasmonic gap-antennas. *Nano Lett.* **14**, 2867–2872. (doi:10.1021/nl500913t)

(7) Shalaev VM. 2007 Optical negative-index metamaterials. *Nature Photon.* **1**, 41–48. (doi:10.1038/nphoton.2006.49)

(8) Dolling G, Enkrich C, Wegener M, Zhou JF, Soukoulis CM, Linden S. 2005 Cut-wire pairs and plate pairs as magnetic atoms for optical metamaterials. *Opt. Lett.* **30**, 3198–3200. (doi:10.1364/OL.30.003198)

(9) Pshenay-Severin E, Hübner U, Menzel C, Helgert C, Chipouline A, Rockstuhl C, Tünnermann A, Lederer F, Pertsch T. 2009 Double-element metamaterial with negative index at near-infrared wavelengths. *Opt. Lett.* **34**, 1678–1680. (doi:10.1364/OL.34.001678)

(10) Klein MW, Enkrich C, Wegener M, Linden S. 2006 Second-harmonic generation from magnetic metamaterials. *Science* **313**, 502–504. (doi:10.1126/science.1129198)

(11) Klein MW, Wegener M, Feth N, Linden S. 2007 Experiments on second-and third-harmonic generation from magnetic metamaterials. *Opt. Express* **15**, 5238–5247. (doi:10.1364/OE.15.005238)

(12) Kim E, Wang F, Wu W, Yu Z, Shen YR. 2008 Nonlinear optical spectroscopy of photonic metamaterials. *Phys. Rev. B* **78**, 113102. (doi:10.1103/PhysRevB.78.113102)

(13) Melentiev PN, Afanasiev AE, Kuzin AA, Baturin AS, Balykin VI. 2013 Giant optical nonlinearity of a single plasmonic nanostructure. *Opt. Express* **21**, 13896–13905. (doi:10.1364/OE.21.013896)

(14) Kruk S, Weismann M, Bykov AY, Mamonov EA, Kolmychek IA, Murzina T, Panoiu NC, Neshev DN, Kivshar YS. 2015 Enhanced magnetic second-

harmonic generation from resonant metasurfaces. *ACS Photon.* **2**, 1007–1012. (doi:10.1021/acsphotonics.5b00215)

(15) Reinhold J, Shcherbakov MR, Chipouline A, Panov VI, Helgert C, Paul T, Rockstuhl C, Lederer F, Kley EB, Tünnermann A, Fedyanin AA, Pertsch T. 2012 Contribution of the magnetic resonance to the third harmonic generation from a fishnet metamaterial. *Phys. Rev. B* **86**, 115401. (doi:10.1103/PhysRevB.86.115401)

(16) Mie G. 1908 Beiträge zur Optik trüber Medien, speziell kolloidaler Metalllösungen. *Ann. Phys. (Berlin)* **25**, 377–445. (doi:10.1002/andp.19083300302)

(17) Ginn JC, Brener I, Peters DW, Wendt JR, Stevens JO, Hines PF, Basilio LI, Warne LK. Ihlefeld JF, Clem PG, Sinclair MB. 2012 Realizing optical magnetism from dielectric metamaterials. *Phys. Rev. Lett.* **108**, 097402. (doi:10.1103/PhysRevLett.108.097402)

(18) Kuznetsov AI, Miroshnichenko AE, Fu YH, Zhang J, Luk'yanchuk B. 2012 Magnetic light. *Sci. Rep.* **2**, 492. (doi:10.1038/srep00492)

(19) Evlyukhin AB, Novikov SM, Zywietz U, Eriksen RL, Reinhardt C, Bozhevolnyi SI, Chichkov BN. 2012 Demonstration of magnetic dipole resonances of dielectric nanospheres in the visible region. *Nano Lett.* **12**, 3749–3755. (doi:10.1021/nl301594s)

(20) Krasnok A, Makarov S, Petrov M, Savelev R, Belov P, Kivshar Y. 2015 Towards all-dielectric metamaterials and nanophotonics. *Proc. SPIE* **9502**, 950203. (doi:10.1117/12.2176880)

(21) Dolgova TV, Maidykovski AI, Martemyanov MG, Fedyanin AA, Aktsipetrov OA, Marowsky G, Yakovlev VA, Mattei G. 2002 Giant microcavity enhancement of second-harmonic generation in all-silicon photonic crystals. *Appl. Phys. Lett.* **81**, 2725–2727. (doi:10.1063/1.1510968)

(22) Leuthold J, Koos C, Freude W. 2010 Nonlinear silicon photonics. *Nature Photon.* **4**, 535–544. (doi:10.1038/nphoton.2010.185)

(23) Shcherbakov MR, Neshev DN, Hopkins B, Shorokhov AS, Staude I, Melik-Gaykazyan EV, Decker M, Ezhov AA, Miroshnichenko AE, Brener I, Fedyanin AA, Kivshar YS. 2014 Enhanced third-harmonic generation in silicon nanoparticles driven by magnetic response. *Nano Lett.* **14**, 6488–6492. (doi:10.1021/nl503029j)

(24) Shcherbakov MR, Vabishchevich PP, Shorokhov AS, Chong KE, Choi D-Y, Staude I, Miroshnichenko AE, Neshev DN, Fedyanin AA, Kivshar YS. 2015 Ultrafast all-optical switching with magnetic resonances in nonlinear dielectric nanostructures. *Nano Lett.* **15**, 6985–6990. (doi:10.1021/acs.nanolett.5b02989)

(25) Shcherbakov MR, Shorokhov AS, Neshev DN, Hopkins B, Staude I, Melik-Gaykazyan EV, Ezhov AA, Miroshnichenko AE, Brener I, Fedyanin AA, Kivshar YS. 2015 Nonlinear interference and tailorable third-harmonic generation from dielectric oligomers. *ACS Photon.* **2**, 578–582. (doi:10.1021/acsphotonics.5b00065)

(26) Staude I, Miroshnichenko AE, Decker M, Fofang NT, Liu S, Gonzales E, Dominguez J, Luk TS, Neshev DN, Brener I, Kivshar Y. 2013 Tailoring directional scattering through magnetic and electric resonances in subwavelength silicon nanodisks. *ACS Nano* **7**, 7824–7832 (doi:10.1021/nn402736f)

(27) Boyd RW. 2003 Nonlinear Optics, 2nd ed. *Academic Press.*

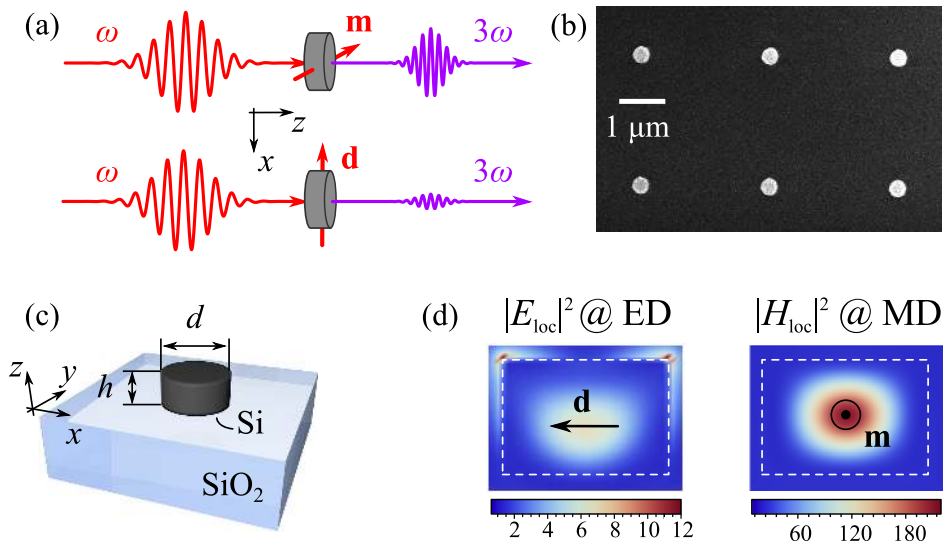

Figure 1: (a) Third-harmonic generation from electric dipolar (**d**) and magnetic dipolar (**m**) resonances of individual silicon nanodisks. (b) A scanning electron micrograph of a sample under study. (c) Schematic representation of the structure under study with dimensions and axes defined. (d) Maps of the local electric field at the ED resonance and magnetic field at the MD resonance proving the multipolar moments of the resonances. The maps are given in the central xz section of the disk for $h = 260$ nm, $d = 360$ nm and $\lambda = 1.030$ and 1.296 μm for the ED and MD resonances, respectively.

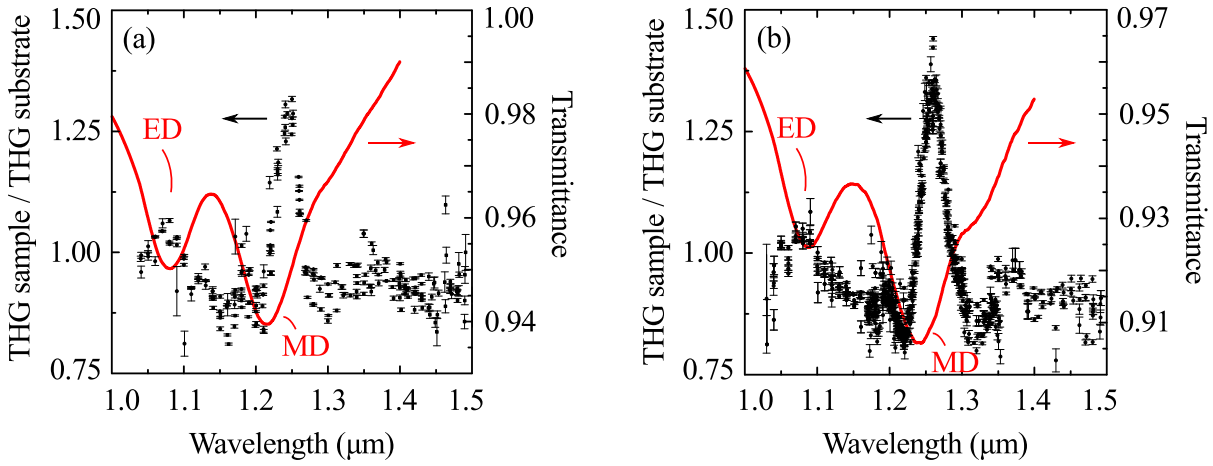

Figure 2: Experimental results. Third-harmonic generation spectra (dots and error bars) and corresponding linear transmittance spectra (red curves) for nanodisks 345 nm (a) and 360 nm (b) in diameter.

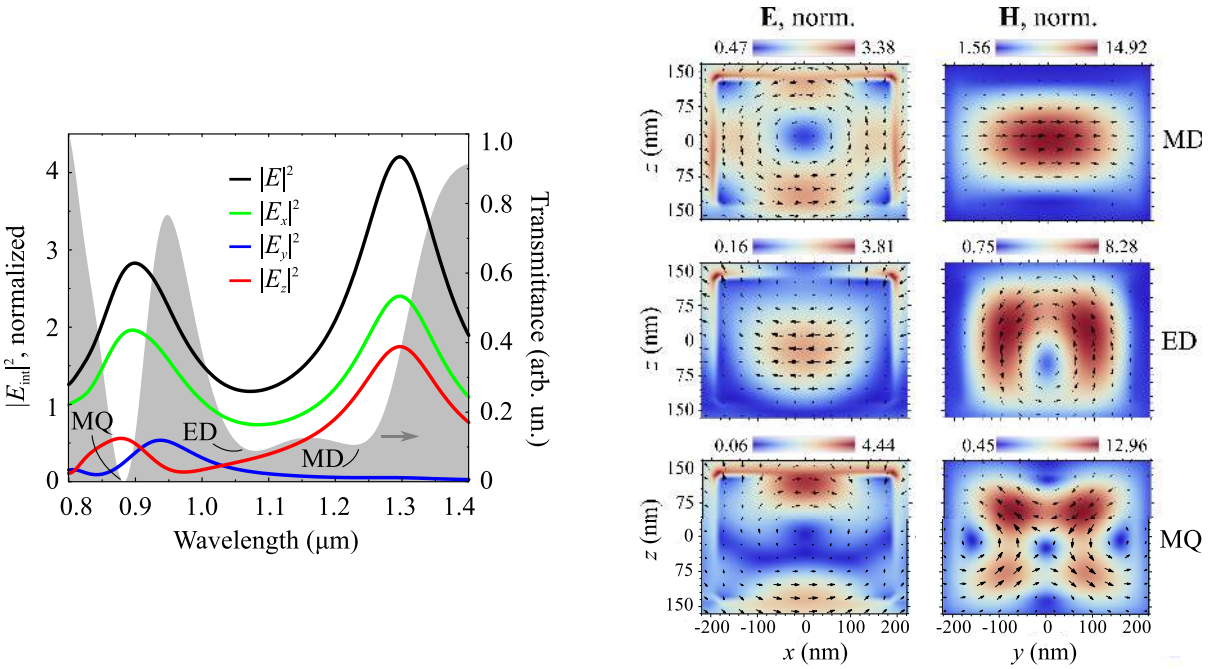

Figure 3: Results of the FDTD numerical calculations. (Left panel) Absolute squared electric field integrated over the volume of the nanodisk; height is 260 nm, diameter is 360 nm. Different field components are indicated with differently colored curves: E_x is given in green, E_y in blue, E_z in red, and total field in black. The gray shaded area denotes the calculated transmittance spectrum. (Right panels) Field distributions in the central sections of the nanodisk at the MD resonance ($\lambda = 1.296$ μm), ED resonance ($\lambda = 1.03$ μm) and MQ resonance ($\lambda = 0.896$ μm).

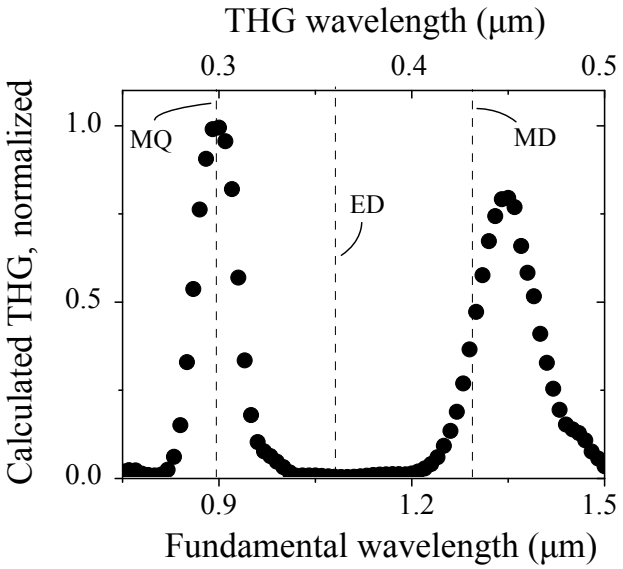

Figure 4: FDTD numerical calculation results for the isolated nanodisk THG response. Nanodisk height and diameter are 260 nm and 360 nm, respectively.